Cross-Link-Governed Dynamics of Biopolymer Networks

Chase P. Broedersz,[1] Martin Depken,[1] Norman Y. Yao,[2] Martin R. Pollak,[3] David A. Weitz,[2,4] and Frederick C. MacKintosh[1]

[1]*Department of Physics and Astronomy, Vrije Universiteit, Amsterdam, The Netherlands*
[2]*Department of Physics, Harvard University, Cambridge, Massachusetts 02138, USA*
[3]*Department of Internal Medicine/Nephrology, Beth Israel Deaconess Medical Center and Harvard Medical School, Boston, Massachusetts, USA*
[4]*School of Engineering and Applied Sciences, Harvard University, Cambridge, Massachusetts 02138, USA*

(Received 5 July 2010; published 30 November 2010)

Recent experiments show that networks of stiff biopolymers cross-linked by transient linker proteins exhibit complex stress relaxation, enabling network flow at long times. We present a model for the dynamics controlled by cross-links in such networks. We show that a single microscopic time scale for cross-linker unbinding leads to a broad spectrum of macroscopic relaxation times and a shear modulus $G \sim \omega^{1/2}$ for low frequencies ω. This model quantitatively describes the measured rheology of actin networks cross-linked with α-actinin-4 over more than four decades in frequency.

DOI: 10.1103/PhysRevLett.105.238101 PACS numbers: 87.16.Ka, 83.80.Lz, 87.15.H−, 87.15.La

Reconstituted biopolymers such as actin are excellent models for semiflexible polymers, with network mechanics and dynamics that are strikingly different from flexible polymer networks [1–8]. One essential feature setting biopolymer networks apart from rubberlike materials is the intrinsic dynamics of their cross-links. Such systems represent a distinct class of polymeric materials whose long-time dynamics are not governed by viscosity or reptation [9], but rather by the transient nature of their cross-links. This can give rise to a complex mechanical response, particularly at long times, where the network is expected to flow. Such flow can have important implications for cells, where their internal networks are constantly remodeling, reflecting the transient nature of their cross-links [10]. The simplest possible description of a material that is elastic on short time scales while flowing on long time scales is that of a Maxwell fluid; this exhibits a single relaxation time τ, as depicted in Fig. 1. Indeed, some recent experiments on transient networks have been modeled with a single relaxation time [11,12]; however, those experiments and others [13,14]—probing longer relative time scales compared to the linker unbinding time—evince a more complex viscoelastic behavior, indicative of multiple relaxation times. Thus, the basic physical principles governing transient networks remain a mystery. A predictive theoretical model is essential to elucidate the effect of dynamic cross-linking and to help explain the reported complex viscoelastic behavior.

Here, we develop a microscopic model for long-time network relaxation that is controlled by cross-link dynamics. This cross-link-governed dynamics (CGD) model describes the structural relaxation that results from many independent unbinding or rebinding events. Using a combination of Monte Carlo simulations and an analytic approach, we demonstrate that this type of cross-link dynamics yields power-law rheology arising from a broad spectrum of relaxation rates. Our predictions are in excellent quantitative agreement with experiments on actin networks with the transient linker protein α-actinin-4.

The CGD model can be qualitatively understood in simple physical terms. We assume each filament is cross-linked to the network, with an average spacing ℓ_c. Only filament bending modes between cross-links can relax (Fig. 1, lower inset), and the thermalization of these results in an entropic, springlike response. To account for transient cross-linking, we assume that the linkers unbind at a rate $1/\tau_{\text{off}}$ (Fig. 1, upper inset), which may depend on temperature [13]. This initiates the relaxation of long-wavelength ($> \ell_c$) modes,

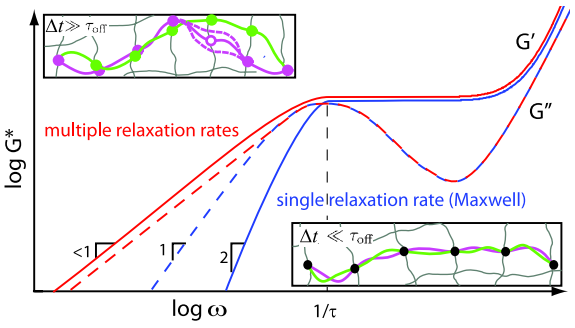

FIG. 1 (color online). A schematic of the frequency dependent shear modulus $G^* = G' + \imath G''$. Nonpermanent networks can exhibit a response ranging from a single time scale (τ) Maxwell-like behavior (blue lines) to a power-law regime with an exponent <1 governed by a broad distribution of relaxation times ($> \tau$) (red lines). Upper inset: For times longer than the unbinding time τ_{off}, large scale conformational relaxation can occur via linker unbinding (open circle) and subsequent rebinding at a new location. Lower inset: For shorter times, only small-scale bend fluctuations between cross-links can relax, resulting in a plateau in G' for frequencies $>1/\tau_{\text{off}}$.

giving rise to a reduced macroscopic modulus. However, the relaxation of successively longer wavelength modes becomes slower, as an increasing number of unbinding events are needed for such a relaxation. This simple physical picture suggests a broad spectrum of relaxation times, as opposed to the single relaxation time of the Maxwell model. As outlined below, both simulations and an analytic treatment of this model yield power-law behavior with $G \sim \omega^{1/2}$ below the characteristic frequency $\omega_0 = 2\pi/\tau_{\rm off}$ [Figs. 2(a) and 2(b)].

We compare the basic predictions of this model to the rheology of a representative transiently cross-linked actin network. As a cross-linker, we use α-actinin-4 [14,15], whose unbinding time $\tau_{\rm off}$ is reported to be in the range 1–10 s. These gels [16,17] exhibit a low-frequency elastic shear modulus G' with a pronounced decay over three decades in frequency, while the viscous modulus G'' exhibits a broad local maximum located near the characteristic frequency of cross-link unbinding [11–13,16,17] [Fig. 2(b)]. In the asymptotic low-frequency range, both moduli exhibit power-law rheology with an approximate exponent of $1/2$, in agreement with our predictions. Such behavior clearly indicates a more complex stress relaxation than captured by the Maxwell model, which is governed by a single relaxation time (Fig. 1). Taken together, the theoretical and experimental results demonstrate a distinct cross-link-governed regime of network dynamics.

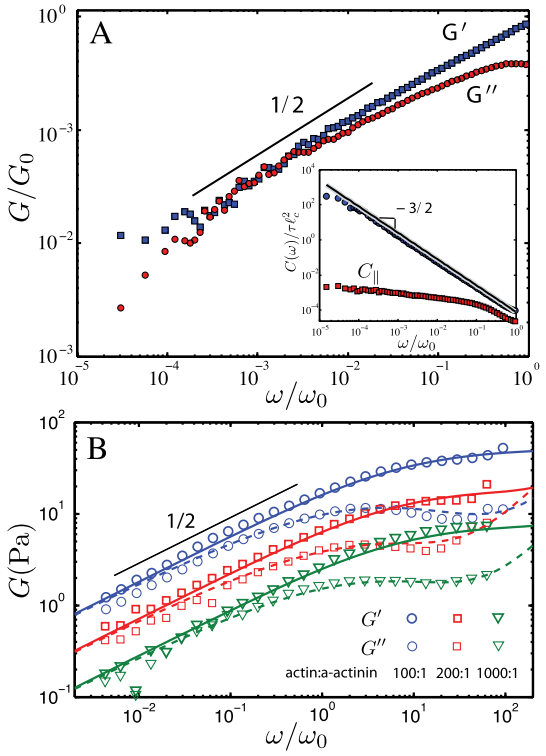

FIG. 2 (color online). (a) The simulated rheology for frequencies below ω_0. The shear modulus is normalized by the elastic plateau value G_0. The inset shows the total power spectrum $C(\omega)$ (blue circles) of distance fluctuations, as well as the fraction $C_\parallel$ coming from effective stretch fluctuations originating in undulations on length scales shorter than the cross-linking distance. The distance fluctuations are determined over a length $16\ell_c$ of a polymer with a persistence length $\ell_p = 32\ell_c$ and a total length $32\ell_c$. The solid black line represents our analytical mean-field CGD prediction. (b) Measured linear rheology of a 23.8 μM actin network cross-linked with various concentrations of α-actinin-4. The low-frequency behavior is consistent with $G \sim (\imath\omega)^{1/2}$. The solid and dashed lines are global fits utilizing our mean-field CGD model for the low-frequency regime together with the known high frequency response [3,4].

To develop a predictive microscopic model, we first consider a single polymer within the network, and then extend the description to the macroscopic level. On length scales longer than ℓ_c, the motion of the polymer is constrained by its cross-linking to the surrounding network (Fig. 1). When a linker unbinds, a local constraint is released, allowing for the relaxation of the freed segment. This thermal relaxation occurs within a time $\tau_{\rm eq}$, which is typically of order milliseconds [3,4,7]. We assume that this process is completed before the segment rebinds to the network at a new location; thus, $\tau_{\rm eq} \ll \tau_{\rm on}$, where $\tau_{\rm on}$ is the rebinding time of the linkers. Furthermore, assuming $\tau_{\rm on} \ll \tau_{\rm off}$, only a small fraction of cross-links will be unbound at any given time, and simultaneous unbinding of neighboring cross-links can be neglected. This suggests a coarse-grained description on length scales $> \ell_c$, in which independent unbinding events occur at a rate $1/\tau_{\rm off}$. Since the relaxation of wavelengths $< \ell_c$ occurs at a much faster rate $1/\tau_{\rm eq}$, we use the wormlike chain model, where the equilibrated short wavelength fluctuations manifest themselves as an entropic stretch modulus $\mu_{\rm th} \sim \kappa^2/\ell_c^3 k_B T$ [2,4]. Here, κ is the bending rigidity, k_B is Boltzmann's constant, and T is the temperature. In this description the coarse-grained energy is given by

$$H_{\rm CG} = \frac{1}{\ell_c}\sum_n \left[\frac{\kappa}{2}|\Delta \mathbf{t}_n|^2 + \frac{\mu_{\rm th}}{2}(|\Delta \mathbf{r}_n| - \ell_c)^2\right], \quad (1)$$

where the sum extends over all cross-link positions $\mathbf{r}_n$, $\mathbf{t}_n$ is the unit tangent vector, and, e.g., $\Delta \mathbf{r}_n = \mathbf{r}_{n+1} - \mathbf{r}_n$.

Using $H_{\rm CG}$, we study the dynamics arising from multiple linker unbinding events, by performing 2D simulations of a single polymer. An initial chain conformation with periodic boundary conditions is randomly drawn from a Boltzmann distribution. Cross-link unbinding events are independent and result in the complete thermal equilibration of the two neighboring polymer segments. This is numerically implemented via a Metropolis Monte Carlo algorithm. These simulations allow us to determine the equilibrium fluctuations of a single polymer, treating its surrounding network as a rigid medium. According to the fluctuation dissipation theorem, the linear mechanical response of the polymer is encoded in the fluctuations of the extension, $\delta\ell$, of the polymer. Interestingly, the simulations demonstrate that the power spectrum $C(\omega) = \langle|\delta\ell(\omega)|^2\rangle$ depends on

frequency as a fractional power law, as shown in the inset of Fig. 2(a), indicating a broad underlying distribution of relaxation times. The exponent is consistent with $-3/2$. Although this exponent also arises in the Rouse model for flexible polymers due to the viscous dynamics of *longitudinal* stretch modes [9], this is not the origin of the behavior found here. Our model does exhibit longitudinal modes; however, their contribution $C_\parallel$ to the full spectrum is subdominant [inset of Fig. 2(a)]. This demonstrates that the polymer's response to an applied tension is dominated by the dynamics of transverse modes.

The dynamical description of a single polymer can be extended to the network level by assuming that the network deforms affinely. The macroscopic shear modulus G^* is then related to the complex response function χ of relative length extension of a single polymer in response to a tensile force: $G^* = \rho/(15\chi)$, where ρ is the length of polymer per unit volume [3,4]. Ignoring end effects, the relative extension $\delta\ell/\ell$ of a polymer segment of length ℓ is conjugate to the uniform tension f, with $\delta\ell(\omega)/\ell = \chi(\omega)f(\omega)$. We use the fluctuation dissipation theorem to calculate the imaginary part of the extensional response function $\ell\chi''(\omega) = \omega\langle\delta\ell^2(\omega)\rangle/2k_BT$. Using a Kramers-Kronig relation, we compute the response function χ and the network shear modulus [18]. Below ω_{off}, the shear modulus depends on frequency as a power law with an exponent of $1/2$ [Fig. 2(a)], consistent with experiments [Fig. 2(b)].

To obtain further insight, we develop a continuum analytical treatment. We calculate the polymer displacement due to the unbinding and subsequent rebinding of a linker to the nth cross-link site. We separate the local equilibration step into a move to the minimum energy position, together with a stochastic thermal contribution set by the form of the energy around the mechanical equilibrium. The mechanical relaxation step $\mathbf{r}_n^{(i)} \rightarrow \mathbf{r}_n^{(\text{meq})}$, from the initial ($i$) position to the local equilibrium position (meq), is determined by

$$\mathbf{0} = \frac{\partial H_{\text{CG}}}{\partial \mathbf{r}_n}\bigg|_{\mathbf{r}_n=\mathbf{r}_n^{(\text{meq})}}. \tag{2}$$

This condition replaces the usual force balance of drag and conservative terms in the low-Reynolds number regime. By performing the discrete calculation solving Eq. (2) and taking the continuum long-wavelength limit, the leading order evolution equations are [17,19]

$$\tau_{\text{off}}\partial_t r_\parallel = \frac{\ell_c^2}{2}\partial_x^2 r_\parallel + \hat{\mathbf{e}}_x \cdot \boldsymbol{\xi}_\perp, \tag{3}$$

$$\tau_{\text{off}}\partial_t \mathbf{r}_\perp = \frac{\ell_c^2}{2}\partial_x^2 \mathbf{r}_\perp + \boldsymbol{\xi}_\perp. \tag{4}$$

Here $\mathbf{r}_\perp$ and $r_\parallel$ are the transverse and longitudinal deflections of the polymer with respect to its average direction $\hat{\mathbf{e}}_x$. The noise $\boldsymbol{\xi}_\perp$ captures both thermal effects and local bucking contributions due to thermally induced compression [17,19]. While thermal contributions can be calculated from a quadratic expansion of H_{CG} around its local mechanical equilibrium, the state of the surrounding polymer influences the form of the Hessian, inducing correlations in the noise. In the inextensible limit, the longitudinal component of $\boldsymbol{\xi}$ is subdominant and is neglected [17,19].

Importantly, the noise $\boldsymbol{\xi}_\perp$ depends nonlinearly on the local state of the polymer and couples Eqs. (3) and (4). To explore this coupling, we artificially reduce the stretch modulus μ. In the limit $\mu \ll \mu_{\text{th}}$, the equations decouple and become exactly solvable; the resulting transverse contribution approaches $C_\perp \sim \omega^{-7/4}$. This can also be seen in our simulations with variable $\mu < \mu_{\text{th}}$ in Figs. 3(a) and 3(b). As μ is reduced below μ_{th}, $C_\perp$ evolves toward $C_\perp \sim \omega^{-7/4}$, which can be seen by the flattening of the normalized spectrum in Fig. 3(b). In the limit $\mu \ll \mu_{\text{th}}$, the transverse bending dynamics are effectively those of a stiff filament fluctuating in a viscous solvent, for which the time-dependent fluctuations are $\langle|\delta\ell(t)|^2\rangle \sim t^{3/4}$ [3,4,20]. Only in this decoupled limit can one understand the dynamics within the framework of an effective viscosity provided by the transient cross-links [19].

The nonlinear nature of the noise $\boldsymbol{\xi}_\perp$ precludes a full analytical solution of the model. Instead, further insight is

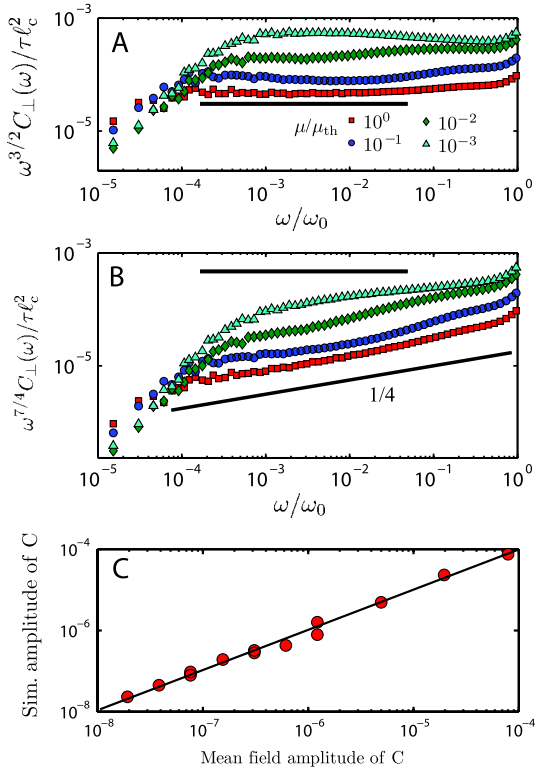

FIG. 3 (color online). The power spectrum $C_\perp(\omega)$ of longitudinal fluctuations originating from transverse undulations on length scales longer than ℓ_c, multiplied with $\omega^{3/2}$ (a) and $\omega^{7/4}$ (b) for a range of polymer backbone compliances. (c) The simulated amplitude of the power spectrum $C(\omega)/\tau\ell_c^2$ plotted against the 2D mean-field prediction for a range of polymer lengths and bending rigidities.

gained by approximating the amplitude of the noise term by its mean-field value calculated from the equilibrium fluctuations of the polymer [19]. In this approximation, the stochastic contributions are uncorrelated in both time and space, resulting in the response function [19]

$$\chi_{\mathrm{MF}}(\omega) \approx 0.0036 \frac{k_B T \ell_c^3}{\pi \kappa^2} \int \frac{dq}{q^2 - 2\imath\omega\tau_{\mathrm{off}}}.$$

This response function captures the cross-link-governed dynamics dominating on time scales $>\tau_{\mathrm{off}}$. Further, we calculate the mean-field correlator, $C_{\mathrm{MF}} \sim \omega^{-3/2}$, in good agreement with the simulations presented in the inset of Fig. 2. As a further test, we perform simulations over a wide range of κ and polymer lengths L; the predicted amplitudes are in excellent agreement with simulated amplitudes, as shown in Fig. 3(c). This further validates the assumptions made in our analytical approach.

To obtain a complete description of the behavior in the experimentally accessible range we include the viscous polymer dynamics in our model [3,4]. This extension relies on the separation of time scales of the fast viscous polymer dynamics and the slow CGD, which implies that their contributions to the fluctuation spectra add in quadrature. The model agrees with the experimental data—over the full range of frequencies—with just three parameters: the plateau modulus, the equilibration time τ_{eq}, and the unbinding time τ_{off} (see Fig. 2). We have globally fitted all data over a decade of cross-linking concentrations with a single value for $\tau_{\mathrm{off}} = 2.7$ s. This provides strong evidence that the low-frequency rheology of actin networks with the physiological linker α-actinin-4 is governed by the linker-controlled dynamics. Furthermore, the fitting procedure yields $\tau_{\mathrm{eq}} < 0.07$ s consistent with $\tau_{\mathrm{eq}} \ll \tau_{\mathrm{off}}$; this, together with the quality of the fit, lends credence to the separation of time scales assumed in our model. Such a separation of time scales also implies that the fluid viscosity does not affect the rheology in the linker-governed regime, consistent with observations in other experiments [11,12]. By contrast, for low enough cross-linking densities τ_{eq} becomes so large that the viscous dynamics and CGD are no longer expected to be well separated. For an expected diffusive propagation of edge effects, we estimate a terminal relaxation time $\tau_r \approx \tau_{\mathrm{off}}(L/\ell_c)^2$ [19]. As few as 10 cross-links per filament can account for the absence of a terminal relaxation in our experiments (Fig. 2). The possibility of observing a terminal relaxation for shorter filaments presents an interesting avenue for future experiments.

Many physiological actin cross-linking proteins are dynamic and should induce a $G^* \propto (\imath\omega)^{1/2}$ behavior at low frequencies. This may enable the cell to regulate its response; on time scales short compared to τ_{off}, the network is effectively permanently connected—thereby providing mechanical resilience—while on longer time scales, dynamic linkers allow for complex network flow. This ability to flow and remodel is required for many vital cellular functions, ranging from motility to division. The extent to which transient cross-linking affects the mechanical properties of the cell is, however, still unknown. Interestingly, some rheological measurements on living cells have suggested a $1/2$ power-law behavior on time scales ranging from several seconds to hours, consistent with our model for transient networks [21,22]. Further experiments are needed to determine whether this regime is due to the transient nature of the cross-links.

This work was funded by FOM/NWO, the NIH (DK59588), the NSF (DMR-1006546), the Harvard MRSEC (DMR-0820484), and the DOE (FG02-97ER25308). We thank G. Barkema for useful discussions.

[1] P. A. Janmey, S. Hvidt, J. Lamb, and T. P. Stossel, Nature (London) **345**, 89 (1990).
[2] F. C. MacKintosh, J. Kas, and P. A. Janmey, Phys. Rev. Lett. **75**, 4425 (1995).
[3] F. Gittes and F. C. MacKintosh, Phys. Rev. E **58**, R1241 (1998).
[4] D. C. Morse, Macromolecules **31**, 7044 (1998).
[5] B. Hinner, M. Tempel, E. Sackmann, K. Kroy, and E. Frey, Phys. Rev. Lett. **81**, 2614 (1998).
[6] M. L. Gardel, J. H. Shin, F. C. MacKintosh, L. Mahadevan, P. Matsudaira, and D. A. Weitz, Science **304**, 1301 (2004).
[7] G. H. Koenderink, M. Atakhorrami, F. C. MacKintosh, and C. F. Schmidt, Phys. Rev. Lett. **96**, 138307 (2006).
[8] R. Tharmann, M. M. A. E. Claessens, and A. R. Bausch, Phys. Rev. Lett. **98**, 088103 (2007).
[9] M. Doi and S. F. Edwards, *The Theory of Polymer Dynamics* (Clarendon, Oxford, 1986).
[10] D. Stamenovic, Nature Mater. **5**, 597 (2006).
[11] O. Lieleg, M. M. A. E. Claessens, Y. Luan, and A. R. Bausch, Phys. Rev. Lett. **101**, 108101 (2008).
[12] O. Lieleg, K. Schmoller, M. Claessens, and A. Bausch, Biophys. J. **96**, 4725 (2009).
[13] S. M. V. Ward, A. Weins, M. R. Pollak, and D. A. Weitz, Biophys. J. **95**, 4915 (2008).
[14] D. Wachsstock, W. Schwarz, and T. Pollard, Biophys. J. **66**, 801 (1994).
[15] H. Miyata, R. Yasuda, and K. Kinosita, Jr., Biochim. Biophys. Acta **1290**, 83 (1996).
[16] N. Y. Yao *et al.* (unpublished)
[17] See supplementary material at http://link.aps.org/supplemental/10.1103/PhysRevLett.105.238101 for methods and theoretical derivations.
[18] The Kramers-Kronig relation involves an integral over the whole frequency domain. Since we only simulate the low-frequency part, we supplement this with the expected plateau above ω_0.
[19] M. Depken *et al.* (unpublished).
[20] R. Granek, J. Phys. II (France) **7**, 1761 (1997).
[21] D. R. Overby, B. D. Matthews, E. Alsberg, and D. E. Ingber, Acta Biomater. **1**, 295 (2005).
[22] N. Desprat, A. Richert, J. Simeon, and A. Asnacios, Biophys. J. **88**, 2224 (2005).